general review of functionalized η^5-Cp complexes including polymer-supported systems, see: Macomber, D. W.; Hart, W. P.; Rausch, M. D. *Adv. Organomet. Chem.* **1982**, *21*, 1.
(4) Reference 1b; for a complete survey of polymer-supported catalysts, see: Pittman, C. U., Jr. In *Comprehensive Organometallic Chemistry*; Wilkinson, G.; Stone, F. G. A., Abel, E. W., Eds.; Pergamon: Oxford; 1983; Vol. 8, 553–611.
(5) For a recent example of polymer modification leading to η^6-arene complexes, see: Andrews, M. P.; Ozin, G. A. *Inorg. Chem.* **1986**, *25*, 2587.
(6) Ford, W. T., Ed. Polymeric Reagents and Catalysts. *ACS Symp. Ser.* **1986**, *308*, 247. Also see: Lieto, J.; Milstein, D.; Albright, R. L.; Minkiewicz, J. V.; Gates, B. C. *CHEMTECH* **1983**, 46.
(7) To our knowledge the only two examples of a characterized transition-metal complex directly attached to a conjugated organic polymer backbone are $Mo(CO)_3$ attached to poly(*p*-phenylene) (yaniger, S. I.; Rose, D. J.; McKenna, W. P.; Eyring, E. M. *Appl. Spectroscopy* **1984**, *34*, 7) and $RhCl_3$, $RuCl_3$, and $PdCl_2$ "attached" to polyphenylene (Ceskoslovenska Akad., Ger. Pat. 2 326 489).
(8) Wright, M. E. *Polym. Prepr. (Am. Chem. Soc., Div. Polym. Chem.)* **1988**, *29*, 294. Wright, M. E. *Organometallics* **1989**, *8*, 407.
(9) Scott, W. J. *Chem. Commun.* **1987**, 1755.
(10) Razuvaev, G. A.; Kuznetsov, V. A.; Egorochkin, A. N.; Klimov, A. A.; Artomov, A. N.; Sirotkin, N. I. *J. Organomet. Chem.* **1977**, *128*, 213.
(11) Negishi, E.; Takahashi, T.; Baba, S.; Van Horn, D. E.; Okukado *J. Am. Chem. Soc.* **1987**, *109*, 2393.
(12) For an example of η^2-alkyne formation, see: Strohmeier, W.; Hellmann, H. *Chem. Ber.* **1965**, *14*, 457. Total carbon monoxide loss has been observed for copolymers containing $\{\eta^6$-arene$\}Cr(CO)_3$ or $\{\eta^5$-Cp$\}Mn(CO)_3$ units at temperatures near 200 °C. Sequential loss or cross-linking was not observed in the systems studied. Some cross-linking was reported for the polymers but it appeared this was a secondary effect of carbon monoxide loss. Pittman, C. U., Jr.; Grube, P. L. *J. Polym. Sci.* **1971**, *9*, 3175. Pittman, C. U., Jr.; Marlin, G. V. *J. Polym. Sci.* **1973**, *11*, 2753. Pittman, C. U., Jr.; Voges, R. L.; Elder, J. *Macromolecules* **1971**, *3*, 302.
(13) Vincent, D. N. *J. Macromol. Sci. Chem.* **1969**, *A-3*, 485.
(14) Graham, J. R.; Angelici, R. J. *Inorg. Chem.* **1967**, *6*, 2082.
(15) Gordon, A. J.; Ford, R. A. *The Chemists Companion*; Wiley: New York, 1972.
(16) Coulson, D. R. *Inorg. Chem.* **1972**, *13*, 121.
(17) King, A. O.; Negishi, E.; Villani, F. J.; Silveira, A. *J. Org. Chem.* **1978**, *43*, 358.
(18) Nast, R.; Grouhi, H. *J. Organomet. Chem.* **1979**, *182*, 197.
(19) Jackson, W. R.; Nichols, B.; Whiting, M. C. *J. Chem. Soc.* **1960**, 469.
(20) Poeth, T. P.; Harrison, P. G.; Long, t. V.; Willeford, B. R.; Zuckerman, J. J. *Inorg. Chem.* **1971**, *10*, 522.
(21) Curtis, M. D.; Allred, A. L. *J. Am. Chem. Soc.* **1965**, *87*, 2554.
(22) Kotlyarevskii, I. L.; Shvartsberg, M. S.; Kruglov, B. G. *Izv. Akad. Nauk SSSR, Otd. Khim. Nauk* **1962**, *184*.

Influence of Molecular Weight on the Thermotropic Mesophases of Poly[6-[4-(4-methoxy-β-methylstyryl)phenoxy]hexyl methacrylate]

Virgil Percec,* Dimitris Tomazos, and Coleen Pugh

Department of Macromolecular Science, Case Western Reserve University, Cleveland, Ohio 44106-2699. *Received November 14, 1988; Revised Manuscript Received January 20, 1989*

ABSTRACT: Poly[6-[4-(4-methoxy-β-methylstyryl)phenoxy]hexyl methacrylate] (4-6-PMA) with different molecular weights and molecular weight distributions was synthesized by group transfer and radical polymerization of the corresponding monomer. The phase behavior of liquid crystalline 4-6-PMA with varying molecular weights was compared to that of its monomeric and dimeric model compounds. The number and nature (i.e., virtual, monotropic, or enantiotropic) of phase transitions were determined by a combination of thermodynamic and kinetic factors. Since the rate of formation of highly ordered phases (crystalline and smectic) decreases with increasing polymer molecular weight, the number and nature of the liquid crystalline phases exhibited by 4-6-PMA vary with increasing molecular weight according to the following trend: monotropic nematic, enantiotropic nematic and enantiotropic smectic, enantiotropic nematic and monotropic smectic, enantiotropic nematic. Phase transition temperatures increase up to a degree of polymerization of about 10–12 and are thereafter essentially molecular weight independent. The rate by which the number of transitions decreases also decreases with increasing polymer molecular weight. However, the enthalpy change associated with the nematic–isotropic transition is molecular weight independent.

Introduction

Why should there be a new investigation concerning the influence of polymer molecular weight on the phase behavior of side-chain liquid crystalline polymers when there are already several such experiments available in the literature?[1-7] The simple reason is that even a recent review article's[8] attempt to discuss this relationship could not answer a number of straightforward questions and, at the same time, raised a series of additional questions.

So far, there is general agreement that an increase of the polymer molecular weight increases mesomorphic–mesomorphic and mesomorphic–isotropic phase transition temperatures up to a certain degree of polymerization, above which they become molecular weight independent.[1-8] However, there is disagreement concerning the exact degree of polymerization above which phase transitions are molecular weight independent. While most of the authors claim that the required degree of polymerization is about 10–12,[3-5,7] results from two research groups consider that it is as high as a few hundred.[1,2,6] Most of the authors claim that the type of mesophase exhibited by a certain polymer is molecular weight independent;[1-5,7] however, a recent publication demonstrates that it too is molecular weight dependent.[6] The dependence of phase transitions on molecular weight led to the conception of the "polymer effect", which assumes that the polymer backbone enhances the tendency of side groups to form mesophases, enlarges the thermal stability of the mesophase, transforms monotropic mesophases into enantiotropic ones, and gives rise to higher ordered mesophases.

The most contradictory issue concerns the influence of molecular weight on the enthalpy changes of mesomorphic phase transitions. Most publications do not report data on this dependence. While one publication reports that this enthalpy change is strongly molecular weight dependent up to degrees of polymerization as high as 400,[1]

0024-9297/89/2222-3259$01.50/0

Table I
Synthesis and Characterization of 4-6-PMA

4-6-MA, mol/L	init, mol/L × 10^3	polymer solvent	polymer yield, %	GPC $\bar{M}_n$	GPC $\bar{M}_w/\bar{M}_n$	phase transitions (°C) and corresponding enthalpy changes (kcal/mru) heating	cooling
				410	1.00	k 50 (8.50) i	i 40 (0.09) n 27 (4.97) k
				805	1.00	k 87 (8.10) i	i 74 (0.16) n 51 (4.50) k
0.295	293.4	THF	65	980	1.09	k 51 (4.14) i[a]	i 43 (0.40) n 1 (0.03) s −14 g
0.295	293.4	THF	65	980	1.09	g −10 s 18 (0.07) n 49 (0.22) i	i 43 (0.40) n 1 (0.03) s −14 g
0.304	123.1	THF	59	2270	1.26	k 68 (2.43) n 82 (o) i[a]	i 67 (0.39) n 28 (0.03) s 1 g
0.304	123.1	THF	59	2270	1.26	g 8 s 34 (0.02) n 74 (0.34) i	i 67 (0.39) n 28 (0.03) s 1 g
0.306	62.5	THF	74	3600	1.35	g 22 s 42 (0.08) n 100 (0.42) i[b]	i 94 (0.49) n 18 (0.03) s 1 g
0.306	62.5	THF	74	3600	1.35	g 22 s 40 (0.04) n 99 (0.42) i	i 94 (0.49) n 18 (0.03) s 1 g
0.310	41.6	THF	73	4310	1.35	g 23 s 41 (0.04) n 102 (0.42) i	i 97 (0.43) n 19 g
0.306	31.1	THF	86	5460	1.26	g 26 s 47 (0.05) n 110 (0.33) i	i 106 (0.44) n 24 g
0.312	24.6	THF	88	6760	1.32	g 29 s 47 (0.06) n 111 (0.38) i	i 106 (0.42) n 24 g
0.292	20.0	THF	74	9590	1.36	g 29 s 49 (0.05) n 104 (0.42) i	i 98 (0.44) n 23 g
0.305	15.6	THF	87	11630	1.36	g 29 n 117 (0.31) i	i 112 (0.38) n 24 g
0.392	17.8[d]	THF	45	12680	1.98	g 29 n 117 (0.34) i	i 113 (0.48) n 24 g
0.490	18.3[d]	Bz	55	14120	2.09	g 29 n 105 (0.28) i	i 99 (0.50) n 23 g
0.490	12.2[d]	Bz	60	27180	2.51	g 29 n 112 (0.39) i	i 107 (0.40) n 24 g
0.245	6.1[d]	THF	67	40500	1.90	g 25 n 100 (0.41) i	i 94 (0.44) n 21 g

[a] Data obtained from the first heating scan. [b] Data obtained from the first heating scan after annealing at room temperature for 60 days. [c] Overlapped transitions, enthalpy changes could not be separated. [d] Radical polymerization, all other polymers were synthesized by group-transfer polymerization.

another claims molecular weight independence up to degrees of polymerization of 40 with an increase above that.[3] Some recent data on side-chain liquid crystalline polysiloxanes showed that, within experimental error, enthalpy changes associated with mesomorphic transitions are molecular weight independent.[7] These data agree with Finkelmann's unpublished results on another series of polysiloxanes.[9] However, polysiloxanes are not the most suitable polymers for this experiment since their mesogenic groups are introduced through polymer homologous reactions which are usually not quantitative; the results are, therefore, susceptible to compositional errors.[8]

In order to help elucidate these unsolved problems, we chose to investigate the influence of molecular weight on the phase transitions and thermodynamic parameters of poly[6-[4-(4-methoxy-β-methylstyryl)phenoxy]hexyl methacrylate] (4-6-PMA) and compare these values to those of its monomeric and dimeric model compounds.

Experimental Section

Materials. Isobutyric acid (99%), 2,4-dimethylglutaric acid (98%, mixture of DL and meso), and tris(dimethylamino)sulfonium difluorotrimethylsiliconate (TASF) (technical grade) were used as received from Aldrich. Dimethylketene methyl trimethylsilyl acetal (MTDA) (95%, Aldrich) was freshly distilled from CaH_2 before use. 2,2′-Azoisobutyronitrile (AIBN) (Fluka) was freshly recrystallized from methanol below 40 °C. Benzene used as a polymerization solvent was first washed with concentrated sulfuric acid and then water, dried over anhydrous $CaCl_2$, refluxed over CaH_2, and then distilled. Tetrahydrofuran (THF) used as a polymerization solvent was refluxed and then freshly distilled from $LiAlH_4$ before each use.

Techniques. ^1H NMR (200-MHz) spectra were recorded on a Varian XL-200 spectrometer. All spectra were recorded in $CDCl_3$ with TMS as internal standard.

A Perkin-Elmer DSC-4 differential scanning calorimeter, equipped with a TADS 3600 data station, was used to determine the thermal transitions which were read as the maximum of the endothermic or exothermic peaks. Unless specified otherwise, all heating and cooling rates were 20 °C/min. Glass transition temperatures (T_g) were read as the middle of the change in the heat capacity. Most thermal transitions were read from second or later heating scans and first or later cooling scans. Second and subsequent heating scans and first and subsequent cooling scans were perfectly reproducible unless stated otherwise. When the second DSC heating scan differed from the first heating scan, the difference will be mentioned, and attempts will be made to explain it. Both enthalpy changes and transition temperatures were determined using indium as a calibration standard. Thermal transition temperatures, their corresponding enthalpy changes, with width of the thermal transition peaks, and the glass transition temperatures reported in Table I are all average values obtained from four to six different sample pans containing approximately 10 mg of polymer. After the first heating scan, each sample was scanned 2 additional times, collecting data from each scan. Therefore, the results tabulated in Table I, including those collected from the first scan, represent the average of four to six data points. The standard deviations of these data are ±0.6 °C for the thermal transitions, ±0.023 kcal/mol for the enthalpy changes, and ±2.6 °C for the width of the thermal transition peaks. However, all the data presented in Table I were rounded off at the last numeral.

A Carl-Zeiss optical polarized microscope (magnification 65×) equipped with a Mettler FP 82 hot stage and a Mettler FP 800 central processor was used to observe the thermal transitions and to analyze the anisotropic textures.[10,11]

Molecular weights were determined by gel permeation chromatography (GPC) with a Perkin-Elmer Series 10 LC instrument equipped with an LC-100 column oven, an LC-600 autosampler, and a Sigma 15 data station. High-pressure liquid chromatography (HPLC) purity determinations were performed with the same instrument. The measurements were made by using a UV detector, THF as solvent (1 mL/min; 40 °C), a set of PL gel columns of 10^2, 5×10^2, 10^3, 10^4, and 10^5 Å, and a calibration plot constructed from polystyrene standards.

Synthesis of Monomers, Model Compounds, and Polymers. 1-[4-(4-Methoxy-β-methylstyryl)phenoxy]hexan-6-ol (4-6-OH) and 6-[4-(4-Methoxy-β-methylstyryl)phenoxy]hexyl Methacrylate (4-6-MA). Both compounds were synthesized as described in a previous publication from our laboratory.[12] 4-6-MA, to be polymerized radically, was purified by recrystallization from methanol. In order to remove protonic impurities from 4-6-MA used in group-transfer polymerizations, the methanol recrystallized monomer was passed through a silica gel column (CH_2Cl_2 as eluent), the solvent removed, and finally the monomer recrystallized from a 9/1 (vol/vol) mixture of cyclohexane and benzene. Monomer purity was always higher than 99.0% (HPLC); mp 53 °C (DSC, 20 °C/min).

Tris(dimethylamino)sulfonium Bifluoride ($TASHF_2$). $TASHF_2$ was synthesized as reported in the literature.[13]

6-[4-(4-Methoxy-β-methylstyryl)phenoxy]hexyl Isobutyrate (M). Its synthesis is outlined in Scheme I. In a 250-mL round-bottom flask equipped with a Dean-Stark trap and a nitrogen inlet–outlet was placed 1.0 g of 4-6-OH (2.9 mmol), 0.26 g of isobutyric acid (2.9 mmol), a trace of *p*-toluenesulfonic acid, and 100 mL of toluene. The reaction mixture was refluxed under

Scheme I
Synthesis of Monomeric (M) and Dimeric (D) Model Compounds of 4-6-PMA

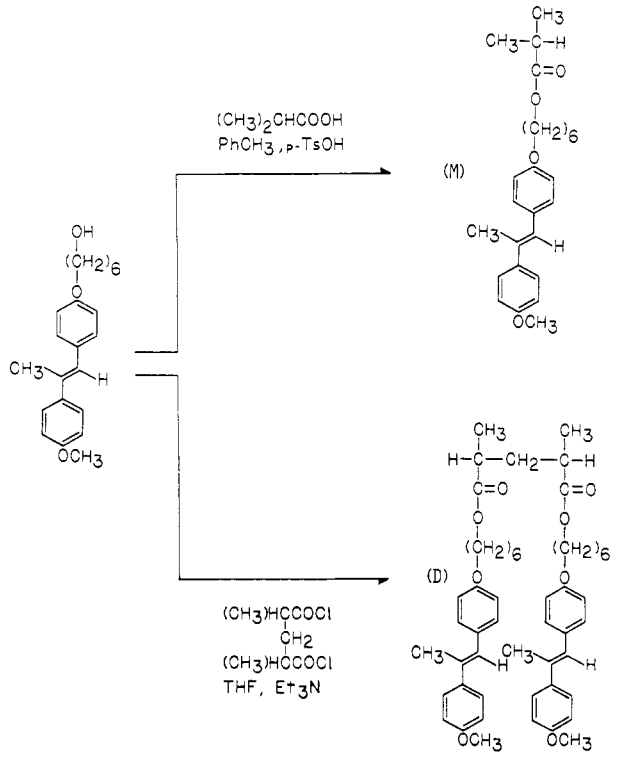

nitrogen until no more dehydration water was collected in the Dean-Stark trap (about 4 h). The reaction flask was cooled to room temperature, and toluene was then removed on a rotary evaporator. The resulting solid was dried, recrystallized twice from methanol, and finally purified by column chromatography (silica gel; CH_2Cl_2 as eluent) to yield 0.61 g (51%) of white crystals; purity >99% (HPLC); mp 50 °C (DSC, 20 °C/min). ^1H NMR ($CDCl_3$, TMS, δ, ppm) 1.83 [m, $-(CH_2)_4-$, 8 protons), 2.26 (s, $CH_3C=$, 3 protons), 2.57 (m, $(CH_3)_2CH$, 1 proton), 3.86 (s, CH_3O, 3 protons), 4.0 (t, CH_2OPh, 2 protons), 4.11 (t, CH_2OOC, 2 protons), 6.71 (s, $PhCH=$, 1 proton), 6.91 (d of d, 2 aromatic protons ortho to methoxy and 2 aromatic protons meta to methyleneoxy), 7.29 (d, 2 aromatic protons meta to methoxy), 7.46 (d, 2 aromatic protons meta to methyleneoxy).

Bis[6-[4-(4-methoxy-β-methylstyryl)phenoxy]hexyl] 2,4-Dimethylglutarate (D). Scheme I outlines the synthesis of D. In a 50-mL round-bottom flask equipped with a condenser and nitrogen inlet–outlet was placed 0.43 g of 2,4-dimethylglutaric acid (2.7 mmol) and 0.19 mL of thionyl chloride (2.7 mmol). The reaction mixture was stirred at 60 °C under nitrogen for 1.5 h, during which time all the acid dissolved. The resulting acid chloride was added dropwise to a stirred solution containing 2.0 g of 4-6-OH (5.9 mmol) and 0.82 mL of triethylamine (5.9 mmol) in 100 mL of dry THF, maintaining the temperature at 0 °C. After the addition, the reaction mixture was left stirring overnight at room temperature. The precipitated Et_3N-HCl was filtered and the solvent removed on a rotary evaporator. The resulting solid was washed with an aqueous solution of $NaHCO_3$ and then water, filtered, dried, and recrystallized twice from methanol. The product was further purified by column chromatography (silica gel, CH_2Cl_2 eluent) to yield 0.72 g (33%) of white crystals; purity >99% (HPLC); mp 87 °C (DSC, 20 °C/min). ^1H NMR ($CDCl_3$, TMS, δ, ppm) 1.17 and 1.20 (d of d, 2 CH_3, 6 protons), 1.49–1.83 (m, 2 $C(CH_2)_4C$ and CCH_2C, 18 protons), 2.26 (s, 2 $CH_3C=$, 6 protons), 4.00 (t, 2 CH_2OPh, 4 protons), 4.11 (t, 2 CH_2OOC, 4 protons), 6.71 (s, 2 $PhCH=$, 2 protons), 6.91 (d, 4 aromatic protons ortho to methoxy and 4 aromatic protons meta to methoxy), 7.46 (d, 4 aromatic protons meta to methyleneoxy).

Radical Polymerization of 4-6-MA. 4-6-PMA of different molecular weights was prepared by radical polymerization of 4-6-MA (Scheme I) in dry benzene or THF using AIBN as initiator at 60 °C for 20 h. Polymerizations were carried out in Schlenk tubes under an argon atmosphere after the monomer solutions were degassed by several freeze–pump–thaw cycles under vacuum. The monomer and initiator concentrations are reported in Table I. After polymerization, the reaction mixture was diluted with more of the same solvent and precipitated into methanol. The filtered polymers were dried under vacuum and then purified by successive reprecipitations from THF into acetone/methanol mixtures and methanol, until GPC chromatograms showed no traces of unreacted monomer or oligomers. The conversions and molecular weights of the purified polymers are presented in Table I together with their thermal characterization.

Group-Transfer Polymerization of 4-6-MA. Group-transfer polymerizations of 4-6-MA were performed in Schlenk tubes under an argon atmosphere at room temperature for 2 h. After the solid monomer was dried further in a Schlenk tube under vacuum overnight, the polymerization tube was filled with argon, and freshly distilled THF was added. The required amount of MTDA was added to the polymerization solution with a microsyringe followed by a small trace of solid $TASHF_2$. After 2 h, the reaction was diluted with THF and precipitated in methanol. The resulting polymers were purified as in the radical polymerizations. Table I summarizes the polymerization conditions, conversions, and characterization of the purified polymers.

Results and Discussion

4-6-PMA with different molecular weights and molecular weight distributions was synthesized by both group-transfer and radical polymerizations (Table I). Although some prior publications used group-transfer polymerization to synthesize side-chain liquid crystalline polymers, they did not report satisfactory control over the resulting polymer molecular weights.[14,15]

Before discussing the current results on the influence of molecular weight on polymer phase transitions, it is necessary to summarize some of our results[12,16-18] and others[14] concerning the influence of the nature of the polymer backbone on the phase transitions of side-chain liquid crystalline polymers. These results are in agreement and are based on the assumption that the flexible spacer provides only a partial decoupling of the motions of the main chain from that of the side groups and that this decoupling increases with increasing flexible spacer length.[19-24] The nature of the highest temperature mesophase is determined by the spacer length and is independent of the nature of the polymer backbone. However, for identical spacer lengths, the nature of the polymer backbone dictates the degree of decoupling and therefore the thermal stability of the mesophase, the number of mesomorphic phases preceding it, and the ease of side-chain crystallization. Flexible backbones tend to give rise to more thermally stable mesophases and simultaneously to an increased ease of side-chain crystallization. Therefore, this effect occasionally leads to the transformation of enantiotropic mesophases into monotropic mesophases in going from a rigid to a flexible backbone. Alternatively, in going from a flexible to a rigid backbone, the tendency toward side-chain crystallization decreases, which may lead to the transformation of virtual mesophases into monotropic or even enantiotropic mesophases. These conclusions are, however, only valid for polymer molecular weights that are high enough for their phase transitions to be molecular weight independent.

The flexibility and therefore the conformational mobility of a polymer backbone are molecular weight dependent, particularly within the range of low molecular weights. Therefore, we may speculate that the phase transitions of a certain polymer should be affected in the same manner by different molecular weights as by different polymer backbone flexibilities.

In order to at least semiquantify this dependence, we must follow the thermal behavior of the model compounds

Scheme II
Synthesis of 4-6-PMA

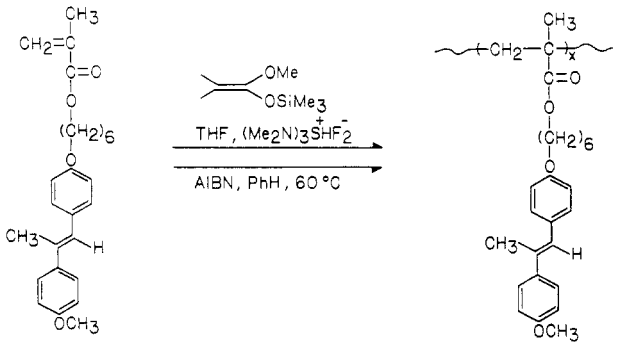

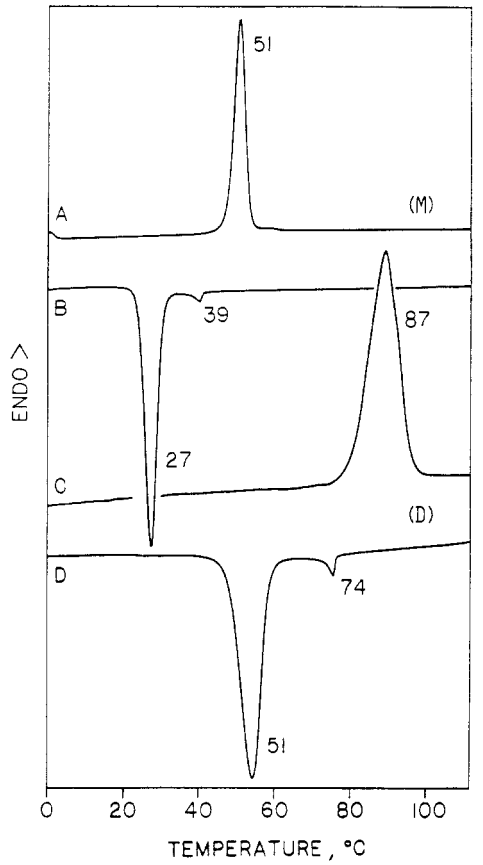

Figure 1. Normalized DSC traces of (A) monomeric unit model (M), first heating scan; (B) monomeric unit model (M), first cooling scan; (C) dimeric unit model (D), first heating scan; and (D) dimeric unit model (D), first cooling scan.

of 4-6-PMA monomeric (M) and dimeric (D) structural units (Schemes I and II) and of several representative 4-6-PMA molecular weights by comparing their DSC scans.

The first heating and cooling DSC scans of the monomeric and dimeric model compounds are presented in Figure 1. Both compounds present a monotropic nematic mesophase. As expected, if the oligomer molecular weight is increased from monomer to dimer, melting, crystallization, and nematic–isotropic transition temperatures increase. Both M and D display only monotropic nematic mesophases independent of their thermal history. Traces A and C of Figure 2 present the first heating and cooling scans respectively of the 4-6-PMA trimer of very narrow molecular weight distribution (Table I) in which a nematic monotropic mesophase and a smectic monotropic mesophase are observed. Because the nematic–smectic transition observed on cooling is located near the glass transition temperature (Figure 2C), smectic phase formation

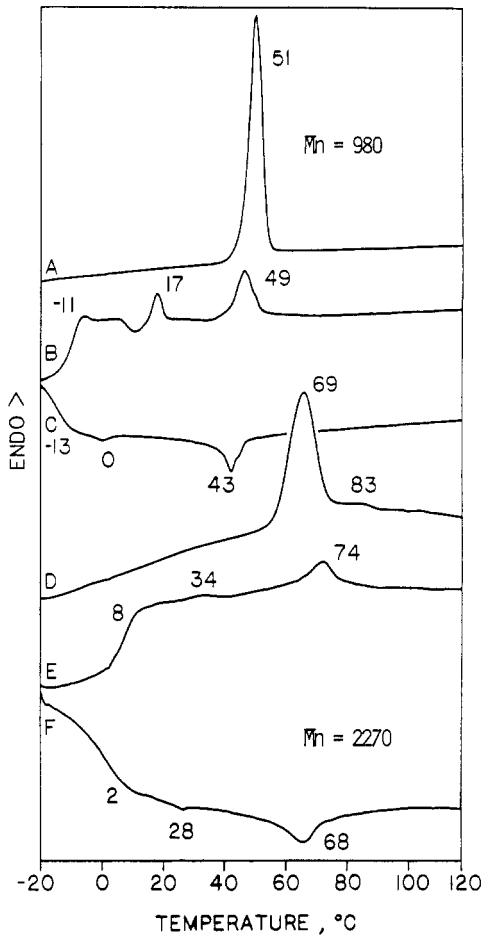

Figure 2. Normalized DSC traces of (A) 4-6-PMA with $\bar{M}_n$ = 980, first heating scan; (B) 4-6-PMA with $\bar{M}_n$ = 980, second and subsequent heating scans; (C) 4-6-PMA with $\bar{M}_n$ = 980, first and subsequent cooling scans; (D) 4-6-PMA with $\bar{M}_n$ = 2270, first heating scan; (E) 4-6-PMA with $\bar{M}_n$ = 2270, second and subsequent heating scans; and (F) 4-6-PMA with $\bar{M}_n$ = 2270, first and subsequent heating scans.

cannot be completed during the cooling process, and an exotherm appears just before the smectic–nematic transition at 17 °C in the next heating scan (Figure 2B). This exotherm is due to the continued transformation of the nematic mesophase into the smectic mesophase. Therefore, when this polymer is cooled below its glass transition temperature, a biphase consisting of an immiscible mixture of smectic and nematic mesophases is frozen.

The nematic–isotropic transition takes place at 49 °C. As seen from the second heating and cooling DSC scans of the 4-6-PMA trimer, both the smectic and nematic mesophases are enantiotropic. However, annealing for a short time within the smectic or nematic mesophase induces very fast crystallization. The first heating scan after crystallization is similar to the first heating scan of Figure 2A. Therefore, both the nematic and smectic mesophases displayed by 4-6-PMA are metastable and are only monotropic under equilibrium conditions. It is interesting to observe that the melting temperature of 4-6-PMA trimer is lower than that of the monomer and dimer model compounds. This is not unexpected since the structure of the trimer obtained by group-transfer polymerization has different chain ends than those of the monomer and dimer model compounds shown in Scheme I.

The main conclusion derived from analysis of these three compounds is that increasing the degree of polymerization from one to two to three raises both the melting and nematic–isotropic transition temperatures. However, crystalline phase transitions are kinetically controlled, while

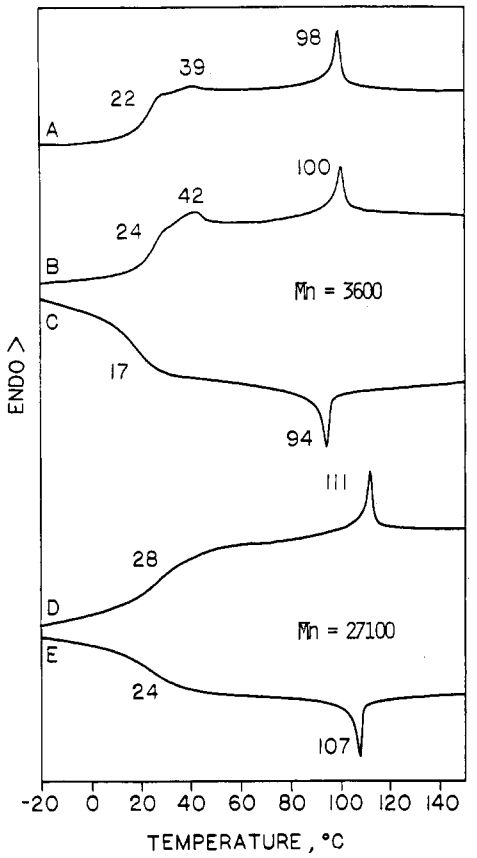

Figure 3. Normalized DSC traces of (A) 4-6-PMA with $\bar{M}_n$ = 3600, second and subsequent heating scans; (B) 4-6-PMA, $\bar{M}_n$ = 3600, first heating scan after sample A was annealed at room temperature for 60 days; (C) 4-6-PMA with $\bar{M}_n$ = 3600, first and subsequent cooling scans; (D) 4-6-PMA, $\bar{M}_n$ = 27 180, second and subsequent heating scans; and (E) 4-6-PMA, first and subsequent cooling scans.

liquid crystalline phase transitions are mainly thermodynamically controlled. Therefore, although an increase in the polymerization degree gives rise to increasing melting transition temperatures, it also decreases the rate of crystallization. Due to this kinetic effect, when the polymer is scanned on both heating and cooling at 20 °C/min, crystallization is depressed so much that it does not appear at temperatures above the oligomer's glass transition temperature. As a consequence, a smectic mesophase, which should be only a virtual mesophase in the case of the monomer and dimer model compounds, is observed with this trimer (Figure 2B,C).

This trend is even clearer if we investigate the first heating and cooling and second heating DSC scans of 4-6-PMA with $\bar{M}_n$ = 2270 (Figure 2D–F). In the first heating scan, the polymer displays a crystalline melting transition at 69 °C, followed by a nematic mesophase that undergoes isotropization at 83 °C. The cooling scan (Figure 2F) displays a nematic mesophase and a smectic mesophase. Therefore, this polymer displays an enantiotropic nematic mesophase and a monotropic smectic mesophase. However, comparison of the second heating scan (Figure 2E) and any cooling scan demonstrates that this polymer exhibits both nematic and smectic enantiotropic mesophases. Again, annealing below the melting point observed in the first heating scan induces polymer crystallization. As a consequence of the higher polymer molecular weight, the crystallization process is even slower than that of the 4-6-PMA trimer. Consequently, under these quasi-equilibrium conditions and as derived from the first scan (i.e., after annealing at room temperature for about 60 days),

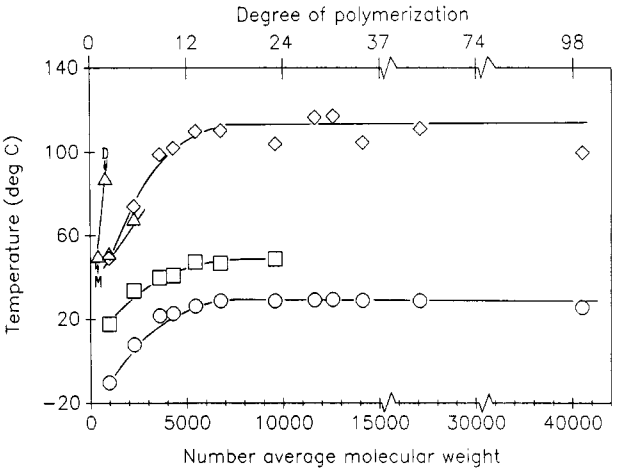

Figure 4. Dependence between (○) glass transition temperature, (□) smectic–nematic transition temperatures, (◇) nematic–isotropic transition temperature, and (△) melting temperature of 4-6-PMA and their number-average molecular weights.

this polymer presents an enantiotropic nematic mesophase and a monotropic smectic mesophase.

The DSC scans of two additional representative polymer molecular weights are presented in Figure 3. 4-6-PMA with $\bar{M}_n$ = 3600 does not exhibit a crystalline melting in the first scan even after lengthy annealing at room temperature. The second DSC heating scan exhibits a glass transition followed by a smectic mesophase which changes into a nematic mesophase at 39 °C. This nematic mesophase undergoes isotropization at 98 °C (Figure 3A). Once annealed at room temperature and cooled below T_g, the subsequent heating scan (Figure 2B) shows a slight change in the temperatures of the smectic–nematic and nematic–isotropic transitions, with additional differences in their enthalpy changes. The major difference is an increase in the enthalpy change of the smectic–nematic transition after annealing (Table I). This is due to the fact that the polymer with this molecular weight does not show a nematic–smectic transition upon cooling or at least does not have a large enough enthalpy change to be observed (Figure 2C). Therefore, most of the nematic–smectic transition takes place upon heating above T_g during the heating scan. In conclusion, 4-6-PMA with $\bar{M}_n$ = 3600 exhibits an enantiotropic nematic mesophase and a monotropic smectic mesophase. However, we should consider that annealing under the most suitable thermal conditions might induce the side-chain crystallization of this polymer. It is, however, certain that this additional increase of the polymer molecular weight kinetically affects not only the crystallization process but also the formation of the smectic mesophase.

This kinetic consequence is further illustrated by the mesomorphic behavior of polymers with higher molecular weights. The second heating and cooling DSC scans of 4-6-PMA with $\bar{M}_n$ = 27 100 are presented in traces D and E of Figure 3. Only an enantiotropic nematic mesophase is observed. The first heating scan is identical with any subsequent heating scan. This is again a kinetic effect. Attainment of an equilibrium situation which would lead to a crystalline polymer would require careful annealing under suitable kinetic conditions, which may involve extended periods of time.

The phase transitions of the entire range of 4-6-PMA molecular weights are summarized in Table I and plotted in Figures 4 and 5. Glass transition, smectic–nematic, nematic–isotropic, and melting transition temperatures all increase with increasing degrees of polymerization (DP) up to DP approximately equal to 12 (Figure 4); the same

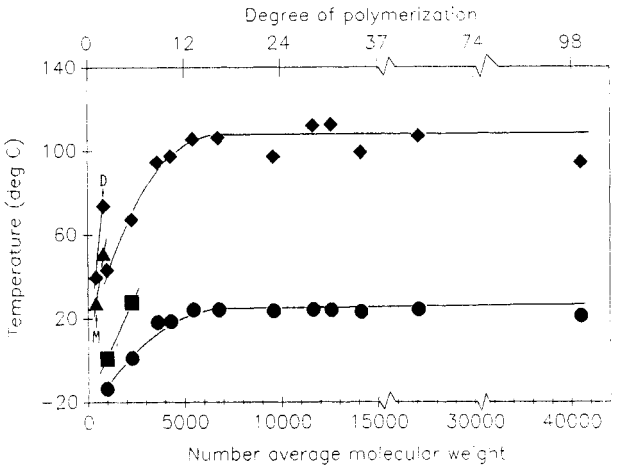

Figure 5. Dependence between (◆) isotropic–nematic transition temperature, (▲) crystallization temperature, (■) nematic–smectic transition temperature, and (●) glass transition temperature of 4-6-PMA and their number-average molecular weights.

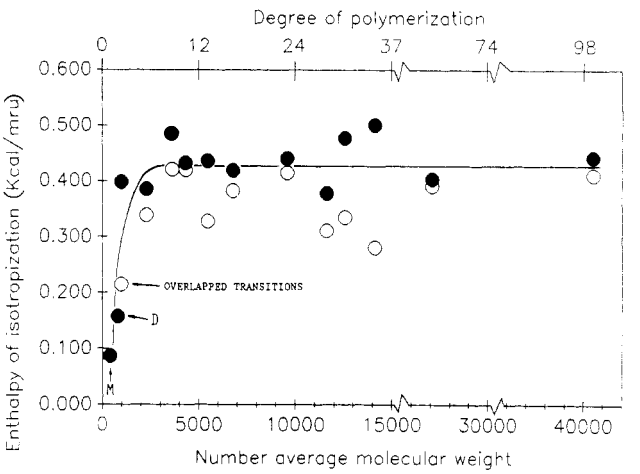

Figure 6. Dependence between the enthalpy of nematic–isotropic (○) and of isotropic–nematic (●) phase transitions and the number-average molecular weight of 4-6-PMA.

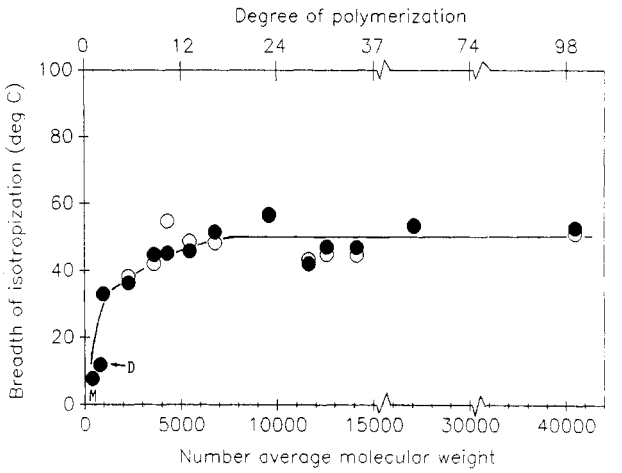

Figure 7. Dependence between the breadth of nematic–isotropic (○) and isotropic–nematic (●) transition peaks and the number-average molecular weight of 4-6-PMA.

is true for the reverse transitions observed on cooling (Figure 5). This is a well-known trend obeyed by any oligomer.[25] The increase of mesomorphic phase transition temperatures with increasing degrees of polymerization has been theoretically explained by Finkelmann et al.[4] The 4-6-PMA molecular weights were determined by GPC calibrated with polystyrene standards and are therefore only relative. Nevertheless, the degree of polymerization of this plateau agrees with that obtained by several authors,[3-5,7] although it disagrees with that determined to be a few hundred,[1,2,6] which is unexpectedly high.[25]

At this point, we can assume that the influence of polymer molecular weight on phase transitions should be considered from both thermodynamic and kinetic viewpoints. The decrease in specific volume at the phase transformation with increasing polymerization degrees raises the phase transition temperatures.[4] This is a thermodynamic trend. However, the rate of formation of each phase decreases with increasing polymerization degrees. This is a kinetic effect. The kinetic influence decreases as the order of the phase under consideration decreases. That is, it decreases in the order crystalline, smectic, nematic. The rate of crystalline phase formation is affected most, and the rate of nematic and glassy phase formations is affected least. This behavior easily explains the trend observed in Figures 4 and 5. The rate of crystalline phase formation is very slow above a certain molecular weight, and therefore a crystalline phase may not form at all during the time scale of our experiments. Due to its close proximity to the glass transition temperature, the smectic mesophase does not form above a number-average molecular weight of 11 630. This molecular weight should be and is higher than that at which the crystalline phase disappears (Table I, Figure 4). If this smectic phase was further separated from T_g, we speculate that it would have been observed even at very high molecular weights. Alternatively and as we have previously shown, when the polymer backbone is very flexible (e.g., polysiloxane backbone), there is no influence of different molecular weights on the number of mesophases observed even when a mesophase is located near T_g.[7] These data agree with that of Finkelmann et al.[4]

We can now make one qualitative comment on the influence of polymer polydispersity on phase transitions. Table I and Figure 4 present thermal transitions for 4-6-PMA with $\bar{M}_n$ = 11 630 ($\bar{M}_w/\bar{M}_n$ = 1.36) and $\bar{M}_n$ = 12 580 ($\bar{M}_w/\bar{M}_n$ = 1.98). For this range of molecular weights, there is no significant difference between the phase transition temperatures of the polymers with broad versus narrow polydispersities.

Consequently, the generally understood meaning of the "polymer effect" should be carefully reconsidered. The polymer backbone does enhance the tendency of low molar mass compounds toward mesomorphism but does so by depressing or even canceling the ability of low molar mass mesogenic compounds to crystallize after polymerization. However, this requires that the monomeric compounds under consideration exhibit at least virtual or monotropic mesophases. This assumption is supported by some recent results which showed that a nonmesogenic disklike monomer does not induce a liquid crystalline mesophase after polymerization.[26] As a consequence of the antagonism between the kinetic and thermodynamic effects discussed above, virtual or monotropic mesophases become enantiotropic upon polymerization. Nevertheless, we must be aware that this might not be the case under thermodynamic equilibrium conditions. This last statement should be carefully considered, particularly when performing physical measurements which require extended periods of time within a mesomorphic phase whose thermal stability range was determined from dynamic experiments.

Figure 6 plots the enthalpy change of the nematic–isotropic and isotropic–nematic transitions as a function of molecular weight. Due to the very low enthalpy change of this transition, the data are quite scattered. The trend, however, is unmistakable. The enthalpy change associated

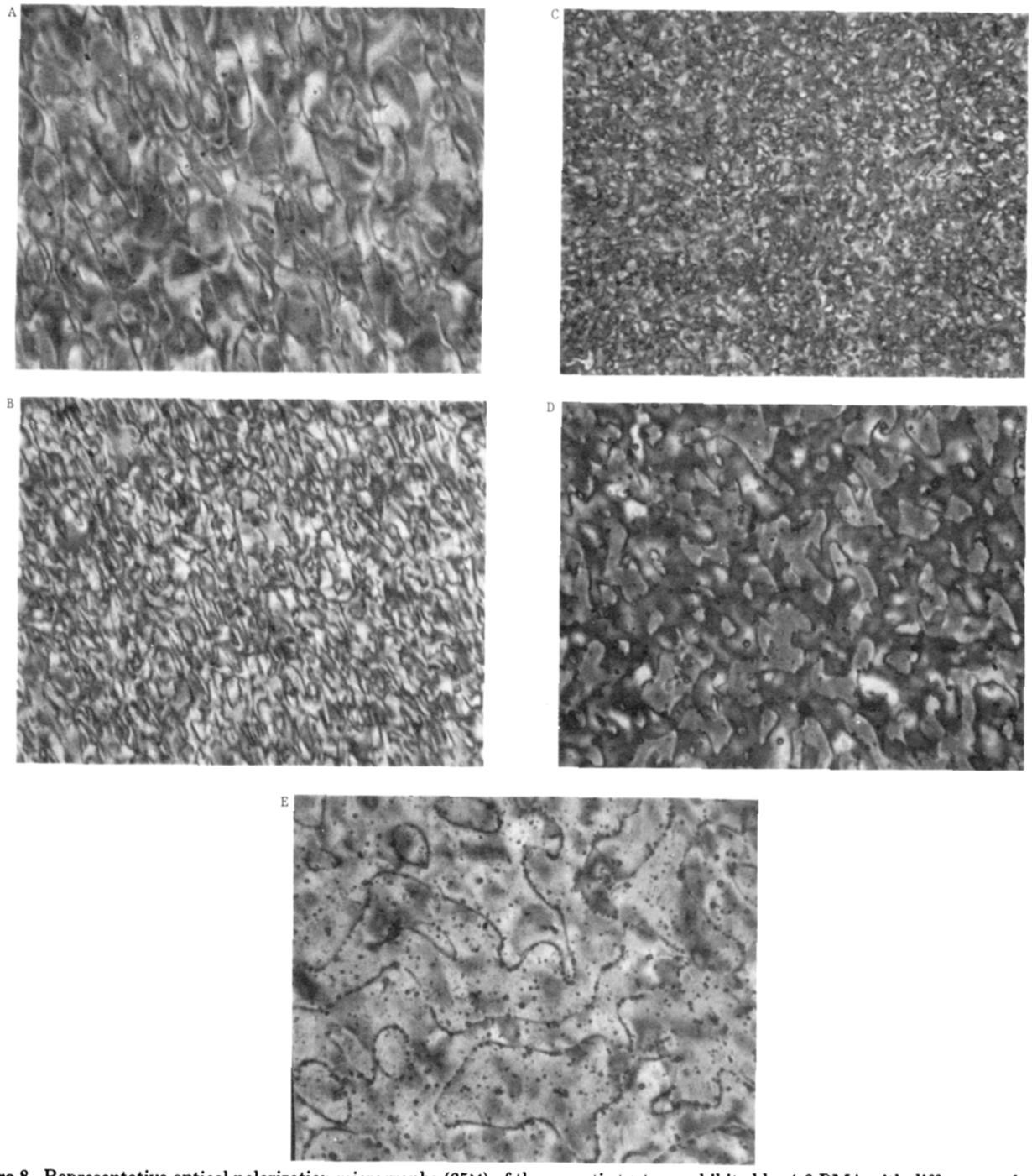

Figure 8. Representative optical polarization micrographs (65×) of the nematic texture exhibited by 4-6-PMA with different molecular weights obtained upon cooling from the isotropic phase with 10 °C/min and annealed for different periods of time: (A) M_n = 6760, after 5 min at 103 °C; (B) M_n = 11 630, after 5 min at 109 °C; (C) M_n = 27 180, after 5 min at 104 °C; (D) M_n = 27 180, after 3 h at 104 °C; (E) M_n = 27 180, after 18 h at 104 °C.

with this transition is molecular weight independent (Table I, Figure 6), although the monomer and dimer model compounds display lower enthalpy changes than the corresponding oligomers and polymers. This is probably due to the slight difference in the structure of their chain ends. This independence of mesomorphic phase transition enthalpy on molecular weight differs from that observed in main-chain liquid crystalline polymers, which follows the same trend as that of their corresponding phase transition temperatures. That is, the transition enthalpy increases with increasing molecular weight up to a certain value, above which it remains constant.[27-29]

Lastly, Figure 7 plots the width of the nematic–isotropic and isotropic–nematic peaks as a function of polymer molecular weight. It is well documented that this parameter provides information about the amount of biphasic material (i.e., isotropic and anisotropic) present at this phase transition.[22] The observed trend is again very clear. This parameter is almost constant; it decreases with decreasing molecular weight only over the range of molecular weights where the phase transition temperatures are molecular weight dependent. This trend is reversed in the case of main-chain liquid crystalline polymers as a result of the higher concentration of chain ends at low degrees of polymerization.[27] However, the peak width of a series of smectic polysiloxanes clearly increased with decreasing degrees of polymerization. This reversed result was explained by the high immiscibility of the backbone and side groups, which decreases with decreasing degree of polymerization.[7]

Finally, we will comment on the influence of molecular weight on the dynamics of mesophase formation as observed by optical polarized microscopy. Figure 8A–C presents several representative optical polarized micrographs as obtained upon cooling the isotropic polymer into the nematic mesophase and annealing within the nematic mesophase for 5 min. The number of inversion lines exhibited by the nematic texture increases with increasing polymer molecular weight. However, upon extended annealing at the same temperature, the number of inversion lines displayed by the high molecular weight polymer's nematic texture decreases (Figure 8C–E), leading to a nematic texture that is similar to that exhibited by the low molecular weight 4-6-PMA after only a short annealing period (Figure 8A,D,E). The coarsening of this nematic phase seems to be related to the dynamics of disclinations,[30-33] which are therefore strongly influenced by the molecular weight of the polymer. The higher the polymer molecular weight, the more the molecular weight kinetic effect slows the dynamics of disclinations. Therefore, the rate of decrease of the number of disclinations per unit volume is very high for low molecular weight polymers and decreases drastically with increasing polymer molecular weight. This behavior must be carefully considered when studying the physical properties of polymers since the number of disclinations per unit volume dictates the size of the nematic "domain".

Before summarizing, it is instructive to discuss the influence of heating and cooling rates on the determination of phase transition temperatures and the corresponding enthalpy changes. Determination of both thermal transition temperatures[34,35] and enthalpy changes[36] by extrapolation to zero heating rate provides true values, eliminating the thermal lag of the DSC cell.[34,37] This effect is particularly important in the determination of crystalline meltings since different heating rates provide different crystal sizes during the reorganization of the polymer crystals.[34,37,38] However, for kinetically controlled phase transitions such as melting and crystallization, extrapolation to zero heating rate does not provide data that correspond to the thermodynamic equilibrium.[38] This requires careful and extensive annealing and extrapolation to both infinite annealing time and infinite molecular weight.[32,38] The time scale of extrapolation to zero heating rate is too short to approach equilibrium. Nevertheless, since liquid crystalline transitions are mostly thermodynamically controlled, data obtained by extrapolation to zero heating rate are more comparable to thermodynamic equilibrium values.[36]

We have characterized several representative polymers with different molecular weights at different heating and cooling rates to determine the effect of extrapolation to zero rate on the various phase transitions and enthalpy changes discussed in this paper. The DSC instrument was calibrated with indium for each scanning rate. Figure 9 presents the extrapolation of the nematic–isotropic and isotropic–nematic transition temperatures for the 4-6-PMA with $\bar{M}_n$ = 27 100, 3600, and 2260. Within instrumental error, the nematic–isotropic and isotropic–nematic transition temperatures extrapolated to zero heating and cooling rates are equal. In all cases, the difference between T_{ni} determined with 20 °C/min and the value obtained by extrapolation to zero heating rate is about 1 °C. This temperature difference is larger on the cooling scan. However, the most important conclusion derived from Figure 9 is that the slopes of the transition temperature–scanning rate plots from either heating or cooling determinations are constant and independent of the molecular

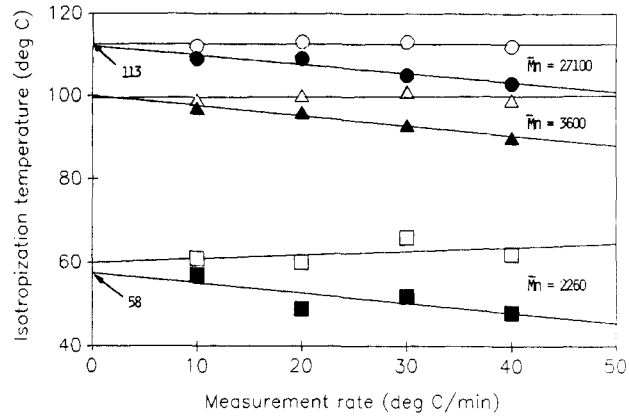

Figure 9. Extrapolation of T_{ni} and T_{in} to zero scanning rate for 4-6-PMA [(○) T_{ni}, (●) T_{in}, $\bar{M}_n$ = 27 100; (△) T_{ni}, (▲) T_{in}, $\bar{M}_n$ = 3600; (□) T_{ni}, (■) T_{in}, $\bar{M}_n$ = 2260).

weight of the polymer sample. Therefore, the trend in transition temperatures plotted in Figures 4 and 5 will not change by extrapolating the data to zero heating and cooling rates.

Plotting the width of the mesomorphic phase transitions and the corresponding enthalpy changes as a function of scanning rate led to the same conclusion. That is, while the extrapolated enthalpic data are certainly more correct, the width of the phase transitions and the corresponding enthalpy changes as a function of polymer molecular weight maintain trends similar to that obtained from measurements at 20 °C/min. Therefore, data from thermodynamically controlled transitions may approximate equilibrium values when they are obtained by extrapolation to zero heating rate.[36] In contrast, although more accurate, extrapolation to zero heating rate of kinetically controlled transitions still provides nonequilibrium data.

In conclusion, these combined thermal and optical results have demonstrated that the influence of polymer molecular weight on phase transitions represents a very delicate relationship between both thermodynamic and kinetic influences. At the present time, we believe that the influence of molecular weight on phase transitions is more complicated for rigid polymer backbones than for flexible backbones, possibly because low and high molecular weight polymers with rigid backbones have highly different chain flexibilities. This results in a kinetic effect similar to that derived from the influence of different polymer backbones having identical mesogenic units and flexible spacers and similar molecular weight on phase transitions.[12,16-18] That is, depending on the flexibility of the polymer backbone as dictated by either the inherent nature of the polymer backbone and/or its molecular weight, a certain mesophase may manifest itself as enantiotropic, monotropic, or virtual.

With inherently flexible polymer backbones such as polysiloxanes, backbone flexibility changes as a function of molecular weight only over the range of very low molecular weights. Therefore, varying the molecular weight has little influence on the nature and number of mesophases exhibited by polymers with very flexible backbones, except when comparing at the level of monomer, dimer, and trimer.[4,7]

Nevertheless, several questions concerning the relationship of molecular weight and liquid crystalline phase behavior have been answered and some previously obtained conclusions reconfirmed. For the polymer system on which the present study is based, when a certain mesophase is observed over the entire range of molecular weights, its thermal transition temperature increases with

increasing degrees of polymerization up to DP = 10–12 and is thereafter essentially molecular weight independent. In contrast, the enthalpy change associated with liquid crystalline phase transitions is molecular weight independent. The dynamics of mesophase formation, including the rate of decrease of the number of disclinations per unit volume and the rate of increase of the size of the nematic "domain", is strongly molecular weight dependent. Both rates decrease with increasing polymer molecular weight.

Acknowledgment. Financial support of this work by the Office of Naval Research and by the Army Research Office is gratefully acknowledged.

Registry No. M, 120411-48-5; D, 120411-49-6; 4-6-PMA, 120416-97-9.

References and Notes

(1) Frosini, A.; Levita, G.; Lupinacci, D.; Magagnini, P. L. *Mol. Cryst. Liq. Cryst.* **1981**, *66*, 21.
(2) Kostromin, S. G.; Talroze, R. V.; Shibaev, V. P.; Plate, N. A. *Makromol. Chem., Rapid Commun.* **1982**, *3*, 803.
(3) Portugall, M.; Ringsdorf, H.; Zentel, R. *Makromol. Chem.* **1982**, *183*, 2311.
(4) Stevens, H.; Rehage, G.; Finkelmann, H. *Macromolecules* **1984**, *17*, 851.
(5) Uchida, S.; Morita, K.; Miyoshi, K.; Hashimoto, K.; Kawasaki, K. *Mol. Cryst. Liq. Cryst.* **1988**, *155*, 93.
(6) Shibaev, V. *Mol. Cryst. Liq. Cryst.* **1988**, *155*, 189.
(7) Percec, V.; Hahn, B. *Macromolecules*, in press.
(8) Percec, V.; Pugh, C. In *Side Chain Liquid Crystalline Polymers*; McArdle, C. B., Ed.; Blackie: Glasgow, 1989; p 30.
(9) Finkelmann, H., private communication.
(10) Demus, D.; Richter, L. *Texture of Liquid Crystals*; Verlag Chemie: Weinheim, 1978.
(11) Gray, G. W.; Goodby, J. W. *Smectic Liquid Crystals. Textures and Structures*; Leonard Hill: Glasgow, 1984.
(12) Percec, V.; Tomazos, D. *J. Polym. Sci., Part A: Polym. Chem.* **1989**, *27*, 999.
(13) Sogah, D. Y.; Hertler, W. R.; Webster, O. W.; Cohen, G. M. *Macromolecules* **1987**, *20*, 1473.
(14) Pugh, C.; Percec, V. *Polym. Prepr. (Am. Chem. Soc., Div. Polym. Chem.)* **1985**, *26*(2), 303.
(15) Kreuder, W.; Webster, O. W.; Ringsdorf, H. *Makromol. Chem., Rapid Commun.* **1986**, *7*, 5.
(16) Percec, V.; Hsu, C. S.; Tomazos, D. *J. Polym. Sci., Polym. Chem. Ed.* **1988**, *26*, 2047.
(17) Percec, V.; Hahn, B. *J. Polym. Sci., Part A: Polym. Chem.*, in press.
(18) Percec, V.; Tomazos, D. *Macromolecules* **1989**, *22*, 1512.
(19) Geib, H.; Hisgen, B.; Pschorn, U.; Ringsdorf, H.; Spiess, H. W. *J. Am. Chem. Soc.* **1982**, *104*, 917.
(20) Spiess, H. W. *Pure Appl. Chem.* **1985**, *57*, 1617.
(21) Boeffel, C.; Spiess, H. W.; Hisgen, B.; Ringsdorf, H.; Ohm, H.; Kirste, R. G. *Makromol. Chem., Rapid Commun.* **1986**, *7*, 777.
(22) Boeffel, C.; Hisgen, B.; Pschorn, U.; Ringsdorf, H.; Spiess, H. W. *Isr. J. Chem.* **1983**, *23*, 388.
(23) Engel, M.; Hisgen, B.; Keller, R.; Kreuder, W.; Reck, B.; Ringsdorf, H.; Schmidt, H. W.; Tschirner, P. *Pure Appl. Chem.* **1985**, *57*, 1009.
(24) Wassmer, K. H.; Ohmes, E.; Portugall, M.; Ringsdorf, H.; Kothe, G. *J. Am. Chem. Soc.* **1985**, *107*, 1511.
(25) Percec, V.; Pugh, C. Oligomers. In *Encyclopedia of Polymer Science and Engineering*, 2nd ed.; Mark, H. F.; Bikales, N. M.; Overberger, C. G.; Menges, G., Eds.; Wiley: New York, 1987; Vol. 10, p 432.
(26) Kohne, B.; Praefcke, K.; Ringsdorf, H.; Tschirner, P. *Liq. Cryst.* **1989**, *4*, 165.
(27) Blumstein, A. *Polym. J. (Tokyo)* **1985**, *17*, 277.
(28) Percec, V.; Nava, H.; Jonsson, H. *J. Polym. Sci., Part A: Polym. Chem.* **1987**, *25*, 1943.
(29) Percec, V.; Nava, H. *J. Polym. Sci., Part A: Polym. Chem.* **1987**, *25*, 405.
(30) Frank, C. F. *Discuss. Faraday Soc.* **1958**, *25*, 19.
(31) Shiwaku, T.; Nakai, H.; Hasegawa, H.; Hashimoto, H. *Polym. Commun.* **1987**, *28*, 174.
(32) Feijoo, J. L.; Ungar, G.; Owen, A. J.; Keller, A.; Percec, V. *Mol. Cryst. Liq. Cryst.* **1988**, *155*, 487.
(33) Rojstaezer, S.; Stein, R. S. *Mol. Cryst. Liq. Cryst.* **1988**, *157*, 487.
(34) Illers, K. H. *Eur. Polym. J.* **1974**, *10*, 911.
(35) Hessel, F.; Herr, R. P.; Finkelmann, H. *Makromol. Chem.* **1987**, *188*, 1597.
(36) Ratna, B. R.; Chandrasekhar, S. *Mol. Cryst. Liq. Cryst.* **1988**, *162B*, 157.
(37) Richardson, M. J. In *Comprehensive Polymer Science*; Sir Allen, G., Ed.; Pergamon Press: Oxford, New York, 1989; Vol. 1, p 867.
(38) Mandelkern, L. In *Comprehensive Polymer Science*; Sir Allen, G., Ed.; Pergamon Press: Oxford, New York, 1989; Vol. 2, p 363.

Detailed Structural Analysis of Polysiloxane Antifoam Agents Using Carbon-13 and Silicon-29 NMR Spectroscopy

I. R. Herbert and A. D. H. Clague*

Shell Research Ltd., Thornton Research Centre, P.O. Box 1, Chester CH1 3SH, England.
Received July 25, 1988

ABSTRACT: Polysiloxane (silicone) antifoam agents are commonly used in the oil industry to reduce or prevent foam formation in nonaqueous systems. In order to improve the understanding of the mechanism of antifoam action, detailed structural analysis of a range of commercially available antifoam agents has been performed by carbon-13 and silicon-29 NMR spectroscopy. Two types of polysiloxanes have been encountered: homopolymers containing methyl(trifluoropropyl)siloxane units and copolymers containing both methyl(trifluoropropyl)- and dimethylsiloxane units. Particular emphasis has been placed on quantitative NMR methods and microstructural analysis of the copolymers.

1. Introduction

The efficiency of processes such as gas/liquid separation can be greatly impaired by unwanted foam or froth formation. Polysiloxane (silicone) antifoam agents are commonly used to reduce or prevent foam formation in nonaqueous systems such as those found in oil production and processing. As part of the study, a range of commercial polysiloxanes were characterized by nuclear magnetic resonance (NMR) spectroscopy to provide a better understanding of the links between molecular structure and performance of antifoam agents. This report describes silicon-29 and carbon-13 NMR methods that have been used to perform detailed structural analysis of typical polysiloxane antifoam agents.

The silicon-containing antifoam agents normally encountered are linear polysiloxanes having the general

0024-9297/89/2222-3267$01.50/0